Spring 2013

Environmental and Physiological Influences on Productivity and Carbon Isotope Discrimination in Eelgrass (*Zostera marina L.*)

Meredith Leigh McPherson
Old Dominion University

ENVIRONMENTAL AND PHYSIOLOGICAL INFLUENCES ON PRODUCTIVITY AND CARBON ISOTOPE DISCRIMINATION IN EELGRASS (*ZOSTERA MARINA* L.)

by

Meredith Leigh McPherson
B.S. May 2009, Old Dominion University

A Thesis Submitted to the Faculty of
Old Dominion University in Partial Fulfillment of the
Requirements for the Degree of

MASTER OF SCIENCE

OCEAN AND EARTH SCIENCES

OLD DOMINION UNIVERSITY
May 2013

Approved by:

Richard Zimmerman (Director)

David Burdige (Member)

Victoria Hill (Member)

Malcolm Scully (Member)

ABSTRACT

ENVIRONMENTAL AND PHYSIOLOGICAL INFLUENCES ON PRODUCTIVITY: IMPACTS ON $\delta^{13}C$ IN EELGRASS (*ZOSTERA MARINA* L.)

Meredith Leigh McPherson
Old Dominion University, 2013
Director: Dr. Richard Zimmerman

Seagrasses' relatively low capacity to exploit HCO_3^- as a source of dissolved inorganic carbon (DIC) for photosynthesis forces them to rely extensively on $[CO_{2(aq)}]$, which is generally low in seawater. As a result, seagrass photosynthesis is generally carbon limited. This study investigated the influence of $CO_{2(aq)}$ transport to RUBISCO, controlled by environmental and physiological mechanisms, on photosynthesis, and the impact on seagrasses $\delta^{13}C$ composition. Light-saturated photosynthesis (P_E) was measured at a variety of flow and DIC regimes to understand carbon uptake at the leaf level, boundary layer conditions, and permeability of the unstirred layer. P_E was saturated with respect to increases in flow above ~2.3 cm s^{-1}. The non-linear response of P_E to $[CO_{2(aq)}]$ was used to predict the maximum physiological photosynthetic rate (P_m). Stable carbon isotope signature ($\delta^{13}C$) for light-saturated conditions was modeled from the theoretical relationship between P_E/P_m and physiological responses to $[CO_{2(aq)}]$ and flow that drive changes in fractionation. Predicted $\delta^{13}C$ for flow saturated, ambient [DIC] was ~7‰, well within the range of reported values for seagrasses. Measured $\delta^{13}C$ values from the Goodwin Islands were lower than predicted light saturated $\delta^{13}C$. However, when historical epiphyte loading was taken into account, $\delta^{13}C$ signatures agreed with published values from similar light-limited environments. The ability to

accurately model productivity and $\delta^{13}C$ of seagrasses suggests a comprehensive understanding of the influence of light, carbon acquisition and environmental conditions on photosynthesis.

Dedicated to

my supportive parents, Pamela and Douglas,

and my love, Arda

ACKNOWLEDGMENTS

As with most things in life, the completion of this thesis would not have been possible without the help of countless individuals who committed their time and energy to my success. Several funding agencies were essential to the completion of this work, including National Science Foundation and Virginia SeaGrant.

First and foremost, I would like to acknowledge my undergraduate and graduate advisor, Dr. Richard Zimmerman for his tireless and enthusiastic guidance over the course of nearly six years. He taught me to think critically and creatively when approaching problem solving, skills that are essential in this field. To him, I owe most all of my relatively extensive field experience in a wide variety of coastal habitats. I am proud to say that Dick has supported me (both financially and professionally) in all of my conference attendances and always encouraged me to gain ample experience presenting and networking. I feel privileged to have had the opportunity to work and learn with Dick, and hope that the completion of my Masters is not the end of our scientific endeavors together.

I would like to express my gratitude towards many additional OEAS faculty members. My thesis committee members, Dr. David Burdige, Dr. Victoria Hill, and Dr. Malcolm Scully, gave essential comments and advice, in which this thesis would not be complete without. I would like to especially thank Dr. Victoria Hill, whose companionship and counseling have been vital to every aspect of this thesis and every other project or publication I worked on for the BORG. Victoria, I know you have great

things ahead. Finally, Dr. Alexander Bochdansky provided critical laboratory space and guidance for all my radioactive carbon isotope experiments.

Of course, BORG members David Ruble, Billur Celebi and Malee Jinuntuya were essential in both the field and lab. I must thank David for not only his great handy work, but for teaching me most of what I know about the bio-optical instruments used the field. Without him, I might still be building my flume or trying to lift the ac-9. I would like to thank Billur and Malee for their unconditional support and the countless discussions that contributed to my understanding and thinking about this research. Field work will never be as fun without you all! I'm looking forward to all that you do in the future.

Last but not least, I would like to thank my family and my fiancé, Arda. For which unconditional support was never a question. I appreciate all the interest in my research, even if you had no idea what I was talking about. Arda, thank you for giving me a shoulder to cry on and a voice of reason. I love you all very much.

TABLE OF CONTENTS

LIST OF TABLES

LIST OF FIGURES

CHAPTER I

INTRODUCTION

Isotopic discrimination against ^{13}C occurs during photosynthetic carbon assimilation can reflect plant metabolic processes and environmental conditions (O'leary 1981). Variations in isotopic composition of terrestrial plants are often attributed to taxon-specific metabolic pathways for carbon acquisition (C_3, C_4, and crassulacean acid metabolism or CAM). Phosphoenolpyruvate (PEP) Carboxylase, the enzyme responsible for the initial carboxylation of CO_2 in C_4/CAM plants is less discriminating against ^{13}C than Ribulose-1,5 Bisphosphate Carboxylase/Oxygenate (RUBISCO), which controls the initial carboxylation step in C_3 phototrophs. These differences cause distinct disparities in isotopic signatures, and terrestrial C_3 plants are typically isotopically lighter (-35‰ to -20‰) than C_4 plants (-15‰ to -9‰) (Smith and Epstein 1971). Unlike terrestrial photosynthesis which depends solely on CO_2 from the atmosphere, aquatic photosynthesis depends on dissolved aqueous carbon dioxide [$CO_{2(aq)}$] (which is not generally present in sufficiently high concentration to satisfy photosynthetic demand in high light environments) and HCO_3^-, a much more abundant form of dissolved inorganic carbon (DIC) in freshwater and seawater. Most aquatic plants (marine alga and some seagrasses) have overcome the photosynthetic limitations imposed by low ($CO_{2(aq)}$) by evolving carbon concentrating mechanisms (CCM) to efficiently utilize HCO_3^- (Madsen and Sand-Jensen 1991). Several studies have explored the influence of CCMs and bicarbonate usage on stable carbon isotope signature ($\delta^{13}C$) because, differences in the

isotopic signatures of source carbon [$CO_{2(aq)}$ (-9‰) and HCO_3^- (0‰) (Raven et al. 2002)] influence isotopic discrimination during carbon assimilation. Utilization of HCO_3^- requires dehydration to $CO_{2(aq)}$ prior to diffusion across the plasma membrane, which can slow the transport of CO_2 to RUBISCO and increase isotopic discrimination (Madsen and Sand-Jensen 1991; Smith and Walker 1980).

Seagrasses, a polyphyletic group of aquatic C_3 angiosperms, are isotopically much heavier than terrestrial C_3 angiosperms (Peterson and Fry 1987). Although stable carbon isotope signatures of seagrass taxa ranges from -23‰ to -3‰ (Hemminga and Mateo 1996), they are typically heavier (-10 ‰) than values reported for marine phytoplankton [-24 ‰; (France 1995)] and marine macroalgae [-20 ‰; (Raven et al. 1995)]. Utilization of HCO_3^- for photosynthesis differs among seagrasses and other marine autotrophs and is likely responsible for some of the disparities in $\delta^{13}C$. Seagrasses typically obtain 50% or less of their inorganic carbon from HCO_3^-, a result of low periplasmic (extracellular) activity of carbonic anhydrase (CA) , the enzyme responsible for the interconversion between HCO_3^- to $CO_{2(aq)}$ at the leaf surface (Beer and Rehnberg 1997; Durako 1993; Invers et al. 2001). Unlike other marine autotrophs, which obtain 80-90% of their inorganic carbon from HCO_3^- (Maberly et al. 1992), the relatively low capacity of seagrasses to exploit HCO_3^- as a source of dissolved inorganic carbon (DIC) for photosynthesis forces them to rely extensively on [$CO_{2(aq)}$], the concentration of which is two orders of magnitude lower than [HCO_3^-]. As a result, seagrass photosynthesis is generally carbon limited in the modern-day ocean (Durako 1993; Zimmerman et al. 1997).

Within individual taxa, the carbon isotope signature in seagrass leaves can be influenced by a variety of environmental and physiological conditions including: 1) the source and concentration of inorganic carbon (Hemminga and Mateo 1996; James and Larkum 1996; Raven et al. 2002); 2) water temperature altering the solubility of $CO_{2(aq)}$ in seawater (Zhang et al. 1995); 3) viscous boundary layers affecting diffusion of $CO_{2(aq)}$ across the leaf-water interface (Hurd 2000; Smith and Walker 1980); and 4) internal carbon concentrating mechanisms, such as recycling of $CO_{2(aq)}$ in the lacuna (Grice et al. 1996).

Light availability influences photosynthetic (and carbon uptake) rates, and several studies inferred a significant positive relationship between $\delta^{13}C$ and light because of the commonly reported negative correlation between seagrass $\delta^{13}C$ and depth (Campbell and Fourqurean 2009; Cooper and Deniro 1989; Grice et al. 1996). Additionally, seasonal changes in productivity due to light availability have been used to explain seasonal trends in $\delta^{13}C$ values (Fourqurean et al. 2005). Isotopic discrimination by RUBISCO drives the underlying mechanism of these patterns, in which kinetic discrimination between $^{13}CO_2$ and $^{12}CO_2$ is lessened at high irradiance when enzymatic demand for CO_2 is high. The variation in seagrass $\delta^{13}C$ due to changes in duration of light saturated photosynthesis was recently placed on a stronger theoretical foundation (Hu et al. 2012). Leaves of *Thalassia testudinum* from Bahamian waters were significantly heavier in ^{13}C relative to plants growing at equivalent depths in Florida Bay because clear, blue waters of the Bahamas allowed more light penetration to greater depths, resulting in higher photosynthetic rates, higher carbon demand, and less isotopic discrimination. More

importantly, the fraction of the day that photosynthesis was light saturated could explain 65% of the isotopic discrimination by RUBISCO across the two locations, regardless of temporal and spatial variations in light availability and quality.

In addition to carbon sources and light availability, water flow is important in structuring boundary layer conditions that influence isotope fractionation in aquatic plants (Smith and Walker 1980). The permeability of inorganic carbon through the unstirred layer [U_p; transport velocity of DIC through the external boundary layer, plus internal leaf structures ($\mu m\ s^{-1}$)] is controlled by physical and physiological conditions. Flowing water increases permeability by reducing the thickness of the unstirred boundary layer around the leaf, in both laminar and turbulent flow conditions (Denny 1993; Hurd 2000). Environmental conditions affecting permeability include temperature, flow, and substrate concentration. Water temperature (controlled by air temperature, solar heat-flux, evaporative cooling, and mixing) has significant influence on the solubility and diffusion of $CO_{2(aq)}$ in seawater and air-sea exchange. Salinity, pH, and alkalinity control the chemical distribution of $CO_{2(aq)}$ and HCO_3^- in the seawater (Zeebe and Wolf-Gladrow 2003), both of which are important carbon sources to seagrasses. Physical changes in temperature affect enzyme kinetics and reaction rates at the site of the two important enzymes responsible for carbon fixation during photosynthesis, CA and RUBISCO. Lastly, biochemical changes in reaction kinetics, pigment membrane structure, and CA concentration play critical roles in influencing the permeability of $CO_{2(aq)}$ and, ultimately, carbon uptake.

Marine angiosperms must overcome many physiological and environmental challenges to survival. High light requirements [>10%; (Duarte 1991)], driven by high physiological demands for dissolved $CO_{2(aq)}$ (Zimmerman et al. 1997; Invers et al. 2001; Palacios & Zimmerman 2007), make seagrasses particularly vulnerable to anthropogenic stresses. Decreases in ocean pH associated with rising atmospheric [CO_2] will likely increase the availability of dissolved inorganic carbon for seagrasses, resulting in increased productivity and reduced light requirements (Palacios and Zimmerman 2007; Zimmerman et al. 1997). Given that global seagrass populations are approaching a state of existential crisis (Orth et al. 2006a), understanding the dynamic relationship between environmental conditions and seagrass physiology that determine carbon uptake is essential for predicting seagrasses response to climate change. This study investigated the effects of water flow, DIC concentration and speciation ($CO_{2(aq)}$ vs. HCO_3^-) on photosynthetic carbon uptake in order to develop a predictive understanding of the impacts of carbon availability on carbon isotope fractionation by *Zostera marina* L (eelgrass). Resulting model predictions were tested against field observations of eelgrass from Chesapeake Bay and compared to previous studies relating $\delta^{13}C$ of turtlegrass (*Thalassia testudinum*, Florida Bay and Banks ex König).

CHAPTER II

METHODS AND PROCEDURE

In order to develop a predictive understanding of the mechanisms driving carbon isotope signatures in seagrass, an integrative approach was taken between theoretical calculations, laboratory experiments and *in situ* observations. Symbols and definitions used here are summarized in Table 1.

Table 1. Summary of symbols, their definitions, and dimensions.

Symbol	Definition	Dimensions
Basic Parameters		
A_T	Total alkalinity	mEq L^{-1}
$A(\lambda)$	Spectral absorptance	Dimensionless
dC	Measured eelgrass carbon uptake	μmol C m^{-2} min^{-1}
$D(\lambda)$	Absorbance [$A = 1\text{-}10^{-D}$]	Dimensionless
$\delta^{13}C$	Isotopic ratio for carbon	‰
E_d	Downwelling plane irradiance	μmol quanta m^{-2} $s^{-1}nm^{-1}$
λ	Wavelength	nm
z	Depth of water column	m
Photsynthetic parameters		
α	Slope of the light limited region of P vs. E curve	μmol C m^{-2} min^{-1}/ m s^{-1}
β	Slope of the flow-limited region of the P vs. u	μmol C m^{-2} min^{-1}/ μmol quanta m^{-2} s^{-1}
P	Realized light-limited photosynthetic rate	μmol C m^{-2} min^{-1}
P_m	Physiological maximum photosynthetic rate	μmol C m^{-2} min^{-1}
PUR	Photosynthetically usable radiation	μmol quanta m^{-2} s^{-1}
Hill-Whittingham parameters (Hill and Whittingham 1955)		
c	Mainstream [DIC]	μM
K_s	Concentration of substrate (CO_2) at ½ P_m	μM
P_E	Light-saturated photosynthesis	μmol C m^{-2} min^{-1}
P_F	Flow-saturated photosynthesis	μmol C m^{-2} min^{-1}

u	Laminar flow velocity	m s^{-1}
U_p	Permeability of the unstirred layer for [DIC]	m s^{-1}
U_pF	Flow-saturated permeability of the unstirred layer	m s^{-1}
U_pCO_2	Permeability of the unstirred layer for $[CO_{2(aq)}]$	m s^{-1}
U_pmin	Minimum permeability at 0 flow	m s^{-1}

Laboratory Experiments

Photosynthesis experiments in the lab on eelgrass collected between the summer of 2011 and 2012 from Goodwin Islands were necessary to parameterize the model developed in this study and predict $\delta^{13}C$ for over a range of environmental conditions (flow and [DIC]).

Light saturated uptake of $^{14}CO_2$ (100 µmol quanta m^{-2} s^{-1}) (Evans et al. 1986; Zimmerman et al. 1991) by eelgrass leaves was measured at 25° C for a range of flow velocities [0 (n = 13); 1 (n = 7); 2 (n = 7); 3 (n = 2); 3.5 (n = 2); 4 (n = 2); and turbulent, nominally 15 cm s^{-1} (n = 9)] in a 1.7 L flume chamber (30 × 6 × 5 cm) constructed of clear polycarbonate (Fig. 1). The second youngest leaves (determined by the order of which leaves emerge from the sheath, inner-most leaf was the youngest) were used for all photosynthesis experiments. Incubation seawater (0.45 µm filtered seawater) was recirculated within the flume using an inline pump, the speed of which was controlled by an AC transformer. Unidirectional laminar flow within the incubation chamber was produced by forcing the water through aeronautical honeycombs (Plascore, Direct Industry) placed at both ends of the chamber. Temperature was separately regulated by a thermostatically controlled circulating water bath system jacketing the recirculating

tubing and connected to an aluminum cooling plate positioned directly under the incubation chamber. All incubations were performed by placing a leaf in the center of the chamber for 15 minutes.

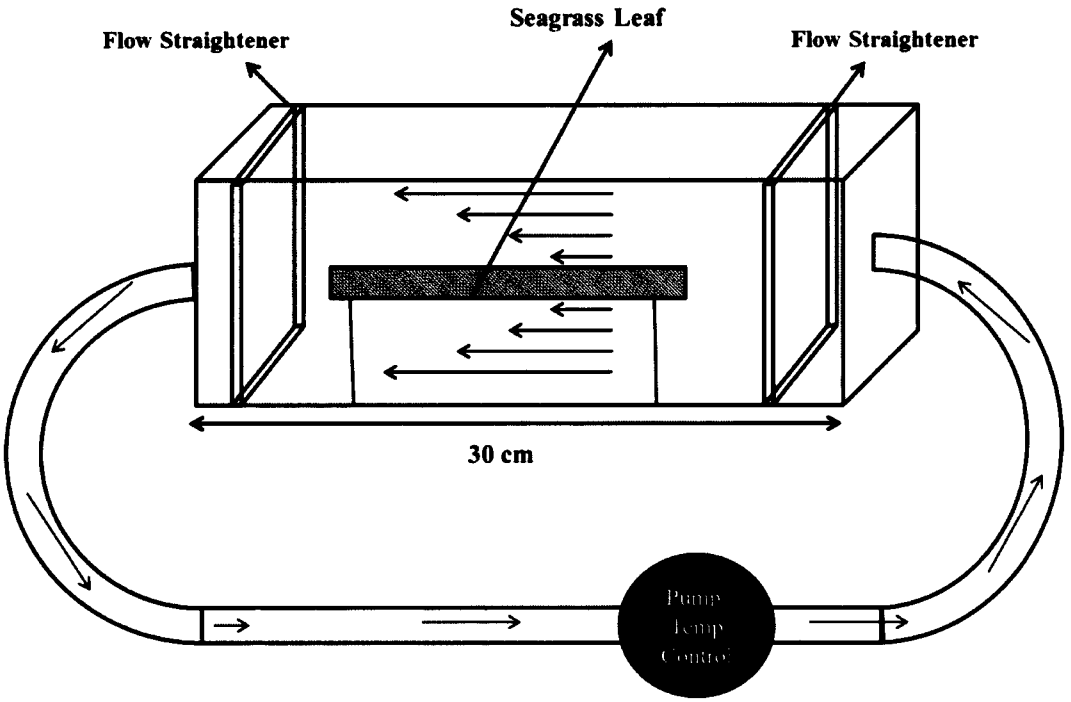

Fig. 1. A diagrammatical representation of the flume setup.

To test the importance of the carbonic anhydrase enzyme for HCO_3^- utilization, and more thoroughly understand carbon uptake mechanisms influencing stable carbon isotope signatures of eelgrass, separate flume incubations were conducted in the presence of 75 μM acetazolamide (AZ, an inhibitor of carbonic anhydrase activity (Bjork et al. 1997; Hellblom and Björk 1999; Invers et al. 1999) at flows of 0, 1, 2, cm s^{-1} and

turbulent (15 cm s^{-}) at ambient [DIC]. The 25 mM AZ stock solution was prepared in 0.05 M NaOH.

Light- and flow-saturated photosynthesis was measured by radioactive carbon uptake over a range of [DIC] (1059 μM to 2534 μM) in a 5 ml water jacketed chamber (Rank Bros.) at 25°C, rather than the flume, because it was easier to manipulate the total [DIC] and seal the chamber without losing CO_2 to the atmosphere or trapping gas bubbles in the flume system. [DIC] in the chamber was manipulated by bubbling with compressed CO_2 to a pH value determined by CO2SYS (ver. 1.05) (Lewis and Wallace 2006), based on the salinity, alkalinity and temperature of the incubation water. Saturating flow in the small chamber was provided by a magnetic stirrer that created a turbulent environment and prevented boundary layer limitation of DIC substrates to the leaf.

Aliquots of 50 and 0.025 μCi L^{-1} of $NaH^{14}CO_3$ (PerkinElmer) were added prior to all incubations in the flume and 5 ml chamber, respectively. At the end of each incubation, the leaves were briefly washed in acidified seawater containing 10% (v/v) HCl for two minutes to remove unincorporated ^{14}C from the external surfaces. Leaves were then ground in NCS tissue solubilizer® using a glass tissue homogenizer and transferred to 20 ml glass vials containing scintillation cocktail (Fisher Scientific Scintiverse™ BD Cocktail 5X18-4). Radioactivity was counted using a Beckman liquid scintillation counter (LS 5000TD). Disintegrations per minute (*dpm*) were corrected for quenching using internal standardization and verified across a range of standard ^{14}C activities prior to experimental runs. Preliminary counts using ^{14}C standards and non-

radioactive leaf homogenates showed no measurable interference (i.e. self-quenching) from leaf pigments or other materials in the tissue homogenates.

Carbon uptake rates were determined from the ratio of ^{14}C incorporated into the leaves (dpm_{sample}) to the total ^{14}C in the incubation medium (dpm_{added}), according to Penhale (1977):

$$P = \frac{dpm_{sample} \cdot [\mathrm{DIC}]}{A \cdot dpm_{added} \cdot t} \qquad (1)$$

where [DIC] was the total dissolved inorganic carbon in the water (after isotopic addition), A was the area (m^2) of the incubated leaf sample, and t was the incubation time. No correction for isotopic discrimination against ^{14}C was applied to carbon uptake calculations because corrections would have been within error estimates of calculated photosynthetic rates. Additionally, control runs with no leaf segments showed there was no significant loss of ^{14}C from the incubation water (by e.g., volitalization, adsorption to the walls of the flume, etc.) during the 15 minute leaf incubations.

Concentrations of $CO_{2(aq)}$, HCO_3^- and total DIC were determined by CO2SYS using the NBS buffer scale from measured values of temperature, salinity, pH, and total alkalinity (TA). Salinity was measured using a refractometer calibrated with deionized water. Incubation medium pH was measured using a Cole Parmer pH/mV/°C meter (Model # 59003-00) and epoxy-body general purpose electrode calibrated using a three point buffer system (Oakton), and NBS buffers. Alkalinity titrations were conducted

prior to each photosynthesis experiment according to (Gieskes and Rogers 1973) by titrating with 0.02N HCl (Fisher Certified 0.0198 to 0.0202N).

Modeling the carbon uptake and isotope fractionation of eelgrass

Predicting Photosynthesis - Prediction of $\delta^{13}C$ requires considerable knowledge of environmental conditions and physiological mechanisms influencing seagrass productivity. The non-linear mathematical relationship between light availability and photosynthesis is well approximated by the commonly used negative exponential function originally developed by Poisson from target theory, and pioneered for photosynthesis by Webb et al. (1974):

$$P = P_E \cdot (1 - e^{-E_d/E_k}) \quad (2)$$

where E_d is the plane irradiance incident on the leaf surface and P_E is the irradiance-saturated rate of photosynthesis. In this light-dependent model, P approaches P_E as E_d approaches the saturation irradiance for photosynthesis, E_k (where $E_k = P_E/\alpha$), and α is the slope of the light limited region of the P vs. E_d curve (Zimmerman et al. 1997).

Most production models assume P_E (as formulated here) to be equivalent to the physiological maximum rate of photosynthesis (P_m), at least with respect to external environmental influences. However, because light saturated photosynthesis of eelgrass

(and most seagrasses) is carbon limited in natural seawater (Beer et al. 2002; Durako 1993; Zimmerman et al. 1997), P_E is actually a variable term that depends on the delivery of CO_2 to RUBISCO, the value of which can be expressed as a square root (hyperbolic) quadratic function of CO_2 concentration and permeability (Hill and Whittingham 1955; Smith and Walker 1980):

$$P_E = \frac{1}{2}\{(K_s U_p + cU_p + P_F) - [(K_s U_p + cU_p + P_F)^2 - 4cU_p P_F]^{\frac{1}{2}}\} \quad (3)$$

where c is the inorganic carbon concentration of the mainstream water (calculated as a function of both [DIC] and [$CO_{2(aq)}$]) and K_s is the half-saturation constant ($CO_{2(aq)}$ concentration) for transport across the leaf structures and assimilation by RUBISCO. The permeability of the unstirred layer (U_p, discussed in detail below), is a proxy for the boundary layer/cellular environment controlling transport of $CO_{2(aq)}$ from the water to the RUBISCO reaction site in the stroma of the chloroplast. P_F represents the maximum rate of photosynthesis under light and flow saturated conditions. A Michaelis-Menton model for enzyme kinetics was fit to measured flow-saturated, carbon-limited photosynthesis over a range of inorganic carbon concentrations using CFTOOL, the Matlab curve-fit tool, as:

$$P_F = P_m \frac{[CO_{2(aq)}]}{K_s + [CO_{2(aq)}]} \quad (4)$$

From Eq. (4), carbon saturated conditions were modeled to obtain P_m. The combination of Eqs. (2) through (4) account for physical, environmental, and enzyme-substrate interactions that control seagrass photosynthesis

All necessary photosynthetic terms were quantified by lab measurements on individual leaves [P_E, E_d, E_k in Eq. (2), and P_F and c in Eq. (3), described above] or from literature values [α (Zimmerman et al. 1997) and RUBISCO K_s = 12 μM (Falkowski and Raven 2007) - Table 5.4].

Permeability of the Unstirred Layer (U_p) - Predicting the stable carbon isotope composition of seagrasses required an understanding of the complex environmental, biochemical, and physiological mechanisms beyond light that affect carbon uptake by aquatic plants. The integrated effects of these processes (except DIC concentration) are aggregated into the term U_p. For a seagrass leaf, this 'unstirred layer' includes the fluid boundary layer (controlled by flow) plus all the structural leaf elements (cell membranes, etc.) that inhibit free movement of $CO_{2(aq)}$ and control the transport and diffusion of $CO_{2(aq)}$ from the leaf surface to the site of fixation by RUBISCO in the stroma of the chloroplast.

Permeability of the fluid + leaf boundary layer was calculated from measures of light saturated carbon fluxes (P_E) over six velocities in the flume. U_p was also determined for light and flow saturated carbon fluxes over five DIC concentrations (discussed below) as:

$$U_p = \frac{dC}{c} \quad (5)$$

where dC was the flux of carbon across the leaf surface and c was the inorganic carbon concentration of the water column, assuming internal leaf concentrations of inorganic carbon were 0 μM under carbon-limited, light-saturated conditions. In order to compare the relative contribution of $CO_{2(aq)}$ and HCO_3^- to leaf photosynthesis, U_p was calculated as a function of $[CO_{2(aq)}]$ (U_pCO_2; Table 1) and [DIC] (U_p) using Eq. (5).

A negative exponential equation, the non-linear curve that produced the best approximation of the influence of flow on permeability, was fit to measured flow-dependent permeability data using CFTOOL, the Matlab© curve fitting tool:

$$U_p = U_{pF} \cdot [1 - e^{-(\beta \cdot u / U_{pF})}] + U_p \min \quad (6)$$

where U_{pF} was the coefficient for flow-saturated permeability, β was the slope of the flow-limiting region of the permeability curve, u was the laminar flow velocity, and $U_p$min represented the diffusive permeability (no turbulent flux) of $CO_{2(aq)}$ across the leaf surface in the absence of flow. To model the effects of [DIC] on permeability of the unstirred layer and photosynthesis, Matlab© coefficients for U_{pF} in Eq. (6) were replaced with calculated values [Eq. (5)] specific to the range of [DIC] tested. Recalculated U_p as a function of increasing water column [DIC] (U_{pF}; based on alkalinity and pH

manipulations) were substituted into Eq. (6) to model permeability across flow and [DIC].

Finally, the range of flow- and inorganic carbon-dependent results for light saturated photosynthesis were substituted into Eq. (2) to model the effect of light, flow, and [DIC] on photosynthesis. The combination of Eqs. (2) through (6) provided the mechanistic basis for predicting the influences of irradiance, flow and [DIC] on photosynthetic rates of the seagrass leaf.

Modeling $\delta^{13}C$ Signature - The stable carbon isotope signature was modeled by constructing a theoretical relationship between $\delta^{13}C$ fractionation and physiological responses to environmental conditions that can drive changes in fractionation, such as light availability, inorganic carbon concentration, and permeability of the unstirred layer. To build the relationship between $\delta^{13}C$ and seagrass carbon uptake rates, light saturated photosynthesis (P_E) was normalized to P_m [light, flow, and CO_2 saturated obtained from Eq. (4)]. At saturating [DIC] and flow ($P_E/P_m = 1$), RUBISCO is not carbon limited and assimilation will fractionate against $^{13}CO_2$, yielding an inherent nominal $\delta^{13}C$ signature representative of RUBISCO's inherent fractionation [-28 ‰; (Falkowski and Raven 2007)]. When P_E is limited by flow, or DIC concentration ($P_E/P_m < 1$), leaf $\delta^{13}C$ will become isotopically heavier, or less negative, because RUBISCO is less able to discriminate against $^{13}CO_2$. The absolute capacity for RUBISCO to discriminate against ^{13}C is also influenced by $\delta^{13}C$ of the DIC source, which is derived from the combined

$\delta^{13}C$ signatures of HCO_3^- ($\delta^{13}C$ = 0‰) and $CO_{2(aq)}$ [$\delta^{13}C$ = -9 ‰ (Kroopnick 1985)] available to the plant (nominally based on source water alkalinity and pH).

$\delta^{13}C$ of Chesapeake Bay Eelgrass

Carbon isotope signatures of naturally occurring eelgrass populations provided a pathway to test model results of predicted $\delta^{13}C$ for a variety of environmental conditions and compare with overall changes in stable carbon isotope signatures as a function of and the daily period of carbon limited (i.e. light-saturated) photosynthesis.

The National Estuarine Research Reserve System (NERRS) site at the Goodwin Islands (Fig. 2; 37° 13' N; 76° 23' W), located at the mouth of the York River, served as the collection and sampling site for *Z. marina*. Samples for natural $\delta^{13}C$ measurements were collected on 15 and 19 July 2011, 15 August 2011, 21 November 2011, and 8 February 2012. Leaf samples were collected at approximately 10 m intervals along a depth gradient (0.1 m to 0.9 m MLW) running NNE from the northern shore of the main island (Fig. 2).

Whole eelgrass shoots were collected for laboratory experiments on 15 August 2011, 8 February 2012, 6 June 2012, and 14 July 2012. Approximately 100 shoots were planted in plastic trays filled with sediment obtained from the Goodwin Islands collection site and placed in 60 L tanks filled with artificial seawater made from Instant Ocean® Sea Salt to a salinity of 18 ppt. Plants were housed inside a greenhouse and exposed to a natural diurnal cycle of UV-filtered sunlight. Tanks were aerated to provide mixing and

prevent boundary limitation of leaf metabolic processes from stagnation of the water column and kept at room temperature (20-25˚C).

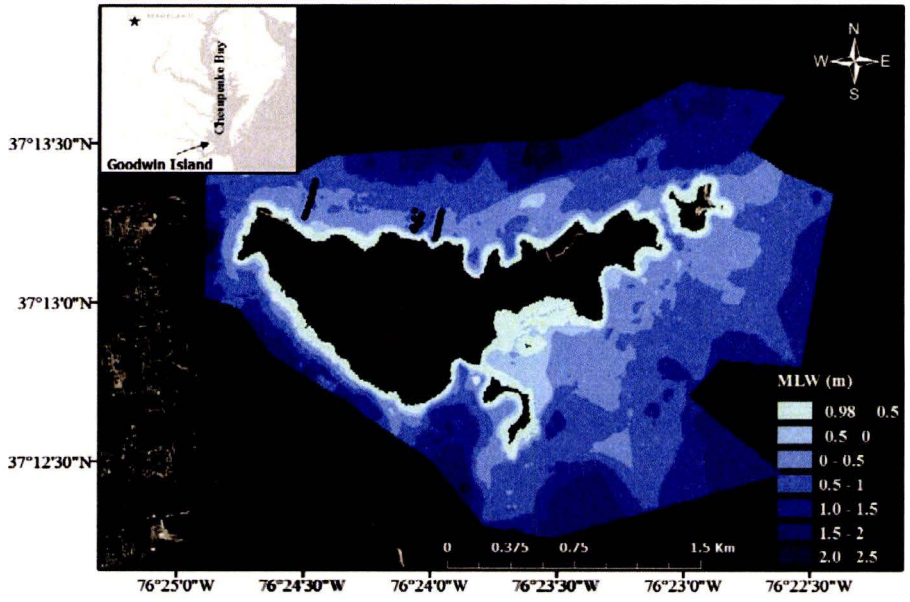

Fig. 2. Bathymetry (MLW) for Goodwin Islands. The black lines depict transects that were performed over a depth gradient within the depth limits for *Z. marina* survival on 15 and 19 July, 15 August , 21 November 2011, and 8 February 2012 at Goodwin Islands, York River (37° 13' N; 76° 23' W).

Seagrass Measurements - Densities of eelgrass along the Goodwin Islands transect were measured by counting all shoots within a randomly positioned quadrat (0.04 m^2) at each $\delta^{13}C$ sampling location. Five representative shoots were harvested from each quadrat for determination of leaf morphology in the laboratory. Lengths of all leaves on the collected shoots were measured to the nearest mm using a flexible tape measure and summed to determine total leaf length for each shoot. Leaf widths were measured to the

nearest 0.1 mm using a digital caliper. The total one-sided leaf area for each shoot (m^2 $shoot^{-1}$) was calculated as the product of total leaf length and leaf width. Leaf area indices (LAI) were calculated for each station as the product of shoot density (shoots m^{-2}) and shoot leaf area (m^2 $shoot^{-1}$).

Leaf $\delta^{13}C$ Measurements - Approximately 25 eelgrass leaves were cleaned of epiphytes by gently scraping with a razor blade. Only healthy, green leaves (1st or 2nd) were kept for $\delta^{13}C$ analysis and were considered representative of recent historical inorganic carbon uptake. Cleaned samples were dried at 80°C, flash frozen in liquid nitrogen and ground to a fine powder in a mortar and pestle and re-dried at 60° C. Carbon isotope composition of the ground leaf samples was analyzed by the University of California Davis isotope facility using standard elemental analyzer isotope ratio mass spectrometer procedures [PDZ Europa 20-20 (Sercon Ltd., Cheshire, UK)]. Samples were combusted at 1000°C in a chromium oxide and silvered copper oxide packed reactor. Oxides were subsequently removed in a reduced copper reactor at 650°C. Carbon isotope ratios were calculated with respect to Vienna Pee Dee belemnite and reported using standard delta notation (‰):

$$\delta^{13}C = [R_{sample} / R_{standard} - 1] \times 1000 \quad (7)$$

where R_{sample} is the $^{13}C/^{12}C$ of the sample and $R_{standard}$ is the $^{13}C/^{12}C$ of Vienna Pee Dee belemnite standard (Sharp 2007).

Goodwin Islands Light Environment - The diffuse attenuation coefficient for downwelling irradiance [$K_d(\lambda)$] from 400 to 700 nm was determined using a diver-operated benthic bio-optical spectroradiometer (DOBBS) consisting of a radiometrically calibrated 3-channel radiometer (*Hydro-Rad 3*; Hobi Labs, Inc) fitted with plane irradiance collectors mounted on an adjustable frame that allowed for the collection of spectral irradiance profiles over a vertical distance of 1.5 m. Profiles were collected on 22 and 24 June 2011, 15 and 19 July 2011, 15 August 2011, 21 November 2011, and 8 February 2012. The instrument was positioned on the seabed over sparse eelgrass within the sampling area. Downwelling spectral irradiance [$E_d(\lambda)$] at the top of the seagrass canopy was measured at a constant location within the transect every 15 minutes for the duration of the collection period. The native spectral distribution is unique for each channel of this instrument (nominally 0.3 nm), and the raw spectra from 400 to 700 nm were resampled to a uniform wavelength increment of 1 nm using a cubic spline. The attenuation coefficient for downwelling plane irradiance [$K_d(\lambda)$] was calculated from the resampled spectra (1 nm resolution) according to Beer's Law:

$$K_d(\lambda) = \frac{-\ln \frac{E_{d1}(\lambda)}{E_{d2}(\lambda)}}{z} \tag{8}$$

where $E_{d1}(\lambda)$ and $E_{d2}(\lambda)$ represent irradiances measured simultaneously by the lower and upper sensors, respectively, separated by a vertical distance (z) of 1 m.

It was important to understand the historical light field experienced by Goodwin Islands eelgrass since incident irradiance reaching the leaf surface influences inorganic carbon assimilation and stable carbon isotope fractionation over the entire leaf growing period, or plastochron interval (~ 2 months; (Hemminga et al. 1999)). Nephelometric turbidity data (NTU) were obtained from the VIMS/NERRS Goodwin Islands continuous water quality monitoring station (YSI Environmental Monitoring System PC6600) for 1 June 2011 to 8 February 2012. Mean daily turbidity data corresponding to *in situ* DOBBS $K_d(\lambda)$ measurements were extracted and a linear regression model was formed between measured $K_d(\lambda)$ and mean daily turbidity. Using a monthly mean turbidity value, this relationship was used to calculate predicted $K_d(\lambda)$ for 4 weeks prior to each sampling day to represent the combined mean lifespan of the first and second leaves used for $\delta^{13}C$ measurements (Hemminga et al. 1999).

Predicting carbon-limited (light-saturated) photosynthesis of Chesapeake Bay eelgrass - The fraction of the day that photosynthesis was carbon limited ($P_{c\text{-}lim,}$ = light saturated) was determined from daily carbon balance estimates using the two-flow radiative transfer model *GrassLight* (Ver. 2.08) (Zimmerman 2003a; 2003b; Zimmerman and Dekker 2006). The model consisted of three separate modules that (i) simulated the architecture, including leaf geometry, of the seagrass canopy and leaf and water column optical properties, (ii) calculated the vertical spectral irradiance distribution within the submerged leaf canopy, and (iii) calculated the seagrass photosynthesis that resulted from spectral light absorption by the leaves. Station-specific values for canopy architecture,

leaf orientation and leaf and historical water column $K_d(\lambda)$ and $E_d(\lambda)$ (described below) were used to initialize the model for each calculation. In addition to predicting carbon limited photosynthesis based on the relationship between measured $K_d(\lambda)$ and water quality parameters (turbidity) , specific light fields for each simulation incorporated the effects of latitude, date, and water depth were also used for comparison. A one-way ANOVA was conducted between model results derived from these two initialization methods. Daily seagrass productivity, driven by the photosynthetically utilized radiation (PUR) captured by the leaves, was calculated by the model assuming the daily variation in irradiance was sinusoidal.

Epiphytes contribute to significant reductions in light availability to submerged aquatic vegetation. Modeling the direct influence on light reduction by epiphytes was achieved using the data of Bulthuis and Woelkerling (1983) (slope = 0.38) in which the relationship between epiphyte coverage (mg cm^{-2}) and absorbance was calculated as:

$$D = 0.379 \cdot L_E \tag{9}$$

where D was the absorbance and L_E was the epiphyte cover (mg DW cm^{-2}). Absorbance was converted to a absorptance ($A = 1 - 10^{-D}$) and incorporated into the radiative transfer model (Zimmerman and Dekker 2006) to attenuate light reaching the leaf surface. Historical data from Moore (2004) reported seasonally variable epiphyte loads experienced by the plant canopy that ranged from 1.2 to 6.3 mg cm^{-2} (Moore 2004).

CHAPTER III

RESULTS

Environmental Influences on Carbon Uptake in Eelgrass

Water flow produced a saturation type response when P_E was measured over a range of velocities in the flume, up to turbulent flow-saturated conditions (Fig. 3A; 0, 1, 2, 3, 3.5, 4, and turbulent; nominally 15 cm s^{-1}). In the presence of AZ, a nonlinear fit of the saturation-type response for the relationship between flow and photosynthesis, and corresponding error estimates for the parameter values, were unobtainable, probably a result of large error estimates. Consequently, the overall effect of external carbonic anhydrase on photosynthetic carbon uptake over a range of flows could not be compared between AZ and non-AZ treatments. However, differences in photosynthesis were investigated at specific flows (0, 1, 2, cm s^{-1} and turbulent) using a 1-way ANOVA. Photosynthesis with the addition of AZ was significantly higher than non-AZ runs at 2 cm s^{-1} (Table 2; $p < 0.05$), but no significant differences were found the other flow conditions (0, 1, 2 cm s^{-1} and turbulent; Table 2; $p > 0.05$).

Table 2. ANOVA comparing photosynthesis measurements at specific flows for flume runs with and without AZ.

Flume Flow (cm s^{-1})	**0 (withAZ)**	**1 (with AZ)**	**2 (with AZ)**	**15(turbulent) (with AZ)**
0 (w/o AZ)	$p > 0.05$			
1 (w/o AZ)		$p > 0.05$		
2 (w/o AZ)			$p < 0.05$	
Turbulent (w/o AZ)				$p > 0.05$

The overall insensitivity of P_E to AZ suggested that periplasmic carbonic anhydrase was not being used by these plants to facilitate DIC uptake and other mechanisms may be exploited to convert HCO_3^- to $CO_{2(aq)}$.

Similarities between photosynthetic rates measured in the presence and absence of AZ in the flume suggested that these plants may have relied heavily on $CO_{2(aq)}$ as an inorganic carbon source. Assuming a constant K_s value across all calculations, separate modeled photosynthetic rates from the Hill-Whittingham equation [Eq. (2)] based on $[CO_{2(aq)}]$ versus total [DIC] ($CO_{2(aq)}+HCO_3^-+CO_3^{2-}$) suggested that plants utilized HCO_3^- and $CO_{2(aq)}$ (Fig. 3A and B). When photosynthesis was modeled using inorganic carbon concentrations equivalent to $[CO_{2(aq)}]$ and calculated U_pCO_2, light and flow saturated photosynthesis was less than one-third of both measured values and Hill-Whittingham modeled photosynthesis using inorganic carbon concentrations equivalent to total DIC (Fig. 3A). The Hill-Whittingham model also predicts a change in the reliance on inorganic carbon species as flume flow increased (Fig. 3B). At zero flow, 78% of inorganic carbon flux across the leaf surface was from $CO_{2(aq)}$, but as photosynthesis reached flow saturation at 3.0 cm s^{-1}, only 42% of total carbon uptake was from $CO_{2(aq)}$.

Calculated permeability through the unstirred layer [U_p in Eq. (5)] also followed the flow-dependent response curve similar to photosynthesis, whether calculated using [DIC] or $[CO_{2(aq)}]$ (Fig. 3C). In this case, a simple negative exponential equation was used to predict U_p for both inorganic carbon source scenarios [Eq. (6)]. U_p calculated using CO_2 (U_pCO_2) sharply increased linearly as a function of flow (slope = 45.4 μm s^{-1}/cm s^{-1}) and saturated at 101 μm s^{-1} (± 4.2) at a flow rate of 2.2 ± 0.05 cm s^{-1}. The initial

slope (β) for U_p calculated using total DIC (U_p) was markedly less steep (slope = 0.2 μm s^{-1}/cm s^{-1}) than U_pCO_2. Additionally, flow saturation and maximum U_p for total DIC (0.9 ± 0.1 μm s^{-1}) occurred at a flow of 4.5 ± 0.2 cm s^{-1} and was 112 times lower than the maximum U_pCO_2.

Measured light and flow saturated photosynthesis (P_F) and calculated maximum permeability [U_{pF}; Eq. (6)] both increased as a function of [DIC] (Fig. 4; R^2 = 0.68 and 0.60, respectively). Thus, P_F and U_p were not completely carbon saturated even at the highest $CO_{2(aq)}$ concentration (1411 μM) employed in this study. However, the curvelinear response of P_F to $CO_{2(aq)}$ predicted P_m (Eq. (4); light, flow, and carbon saturated) to saturate at 15000 μM $CO_{2(aq)}$ and a photosynthetic rate of 196 μmol C m^{-2} min^{-1}. P_F increased 9-fold, while U_{pF} linearly increased 4-fold as DIC increased from 1058 μM (pH = 8.2) to 2534 μM (pH = 6.0). Using calculated U_{pF} [Eq. (6); U_p] and corresponding DIC concentrations, modeled flow versus permeability (Fig. 5A) and photosynthesis curves (Fig. 5B) were constructed. The linear slope for flow-limited photosynthesis (μmol C m^{-2} min^{-1}/cm s^{-1}) increased from 9.9 (SE ± 0.67) to 41.0 (SE ± 1.4) between DIC concentrations of 1058 μM to 2534 μM. The observed 9-fold increase in P_F from low to high [DIC] treatments was most likely due to large increases in available [$CO_{2(aq)}$] to the plant (150-fold increase) and not likely from an increase in total HCO_3^- (2-fold increase) or permeability of the unstirred layer (3-fold increase; Fig. 5).

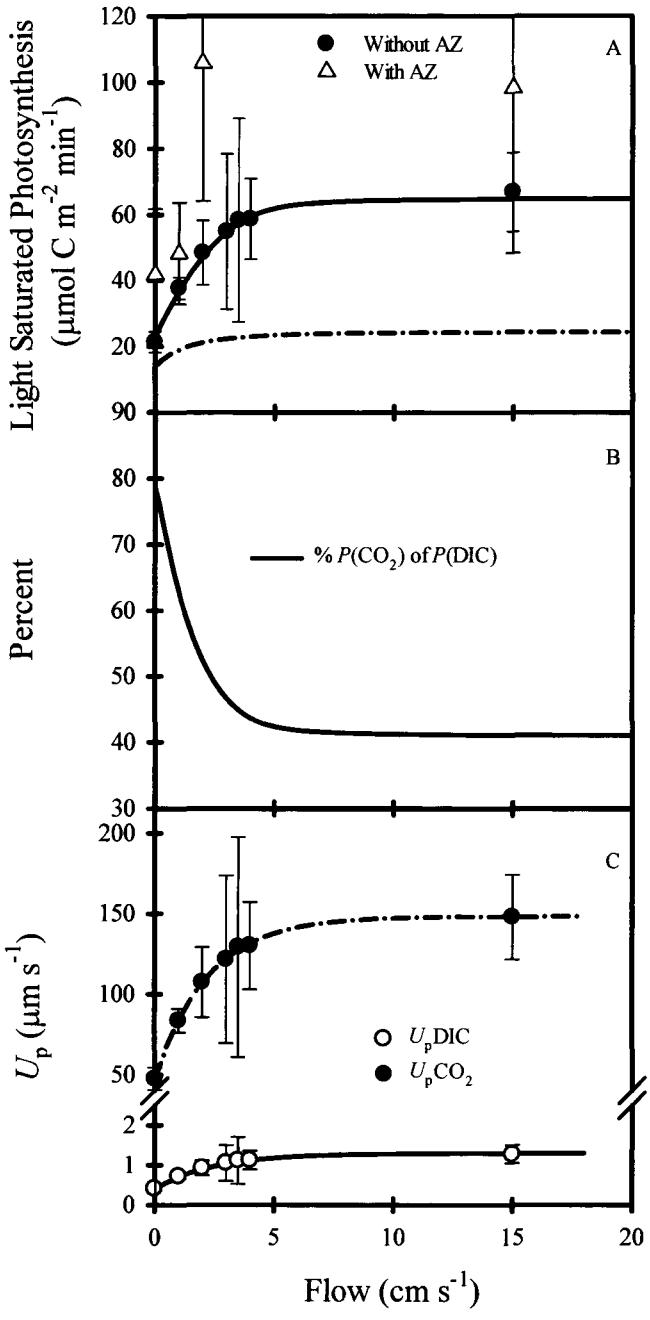

Fig. 3. A) Measured photosynthesis (symbols, ± 1 SE, n = 66), with and without acetezolemide (AZ). Modeled photosynthesis without AZ, for K_s = 12 μM (Falkowski and Raven 2007), calculated from total [DIC] using the Hill-Whittingham quadratic equation [Eq. (3)] plotted as a function of flow (solid line). Modeled photosynthesis without AZ plotted as a function of flow for Hill-Whittingham calculations based on bulk flume [$CO_{2(aq)}$], for K_s = 12 μM, (dash-dot line). B) The flow dependence of

Fig. 3. Continued. photosynthesis on inorganic carbon species shown as the percent of photosynthesis calculated using $[CO_{2(aq)}]$ to photosynthesis calculated using DIC from the Hill-Whittingham equation. C) Calculated permeability of the unstirred layer calculated using bulk [DIC] (solid line; U_pDIC) and $[CO_{2(aq)}]$ (dash-dot line; U_pCO_2) plotted as a function of flow. The curve represents a negative exponential regression $\{U_p = U_{pF} \cdot [1 - e^{-(\alpha \cdot u / U_{pF})}] + U_p \text{ min}\}$ fit to $CO_{2(aq)}$ and DIC calculated data ($R^2 = 0.989$ and $R^2 = 0.996$, respectively).

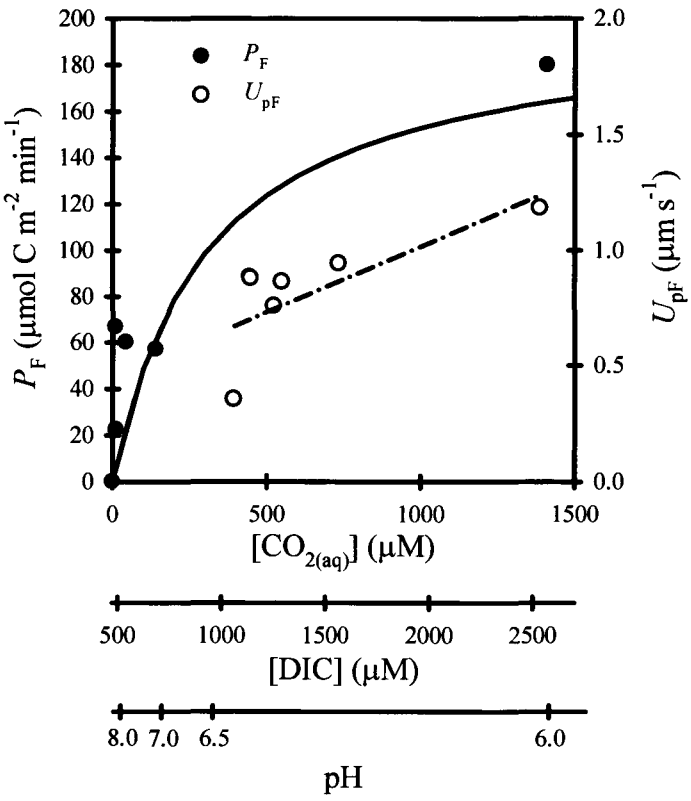

Fig. 4. Measured light and flow saturated photosynthesis (P_F; $R^2 = 0.67$; $P_F = 200 \cdot [CO_{2(aq)}]/308 + [CO_{2(aq)}]$) and calculated maximum permeability of the unstirred layer (U_{pF}; $R^2 = 0.60$; $U_{pF} = 0.0004 \cdot [DIC] + 0.26$) plotted as a function of $[CO_{2(aq)}]$, [DIC], and pH.

The three-dimensional representation of realized photosynthesis (P) was markedly different between ambient and enriched [DIC] (DIC = 1059 and 2534 μM, respectively; Fig. 6A and B). By definition, photosynthesis for both DIC conditions was zero across all flows in the dark ($E = 0$). At zero flow, $[CO_{2(aq)}]$ was responsible for a doubling in the threshold for irradiance saturation (flow dependent $CO_{2(aq)}$ use shown in Fig. 3B; E_k = 7 and 15 μmol quanta m^{-2} s^{-1}) between the two DIC treatments (Fig. 6A and B) because large changes in $[CO_{2(aq)}]$ allowed for more molecules to diffuse across the leaf surface . However, light-saturated photosynthesis increased for both ambient and high DIC treatments at flow-saturated conditions (u = 20 cm s^{-1}; E_k = 18 and 57 μmol quanta m^{-2} s^{-1}, respectively). The irradiance required to saturate photosynthesis (E_k) increased with flow because turbulent flux of [DIC] into the boundary layer increased as a function of flow. Therefore, at high flow regimes, the onset of carbon-limited photosynthesis was delayed. Photosynthesis reached maximum rates for ambient DIC conditions (~1290 μM) and became flow and light saturated when $u > 3$ cm s^{-1} and $E > 40$ μmol quanta m^{-2} s^{-1}. The ability to model photosynthesis based on varying light, flow, and [DIC] indicated a mechanistic path for predicting environmental effects on carbon uptake in seagrasses.

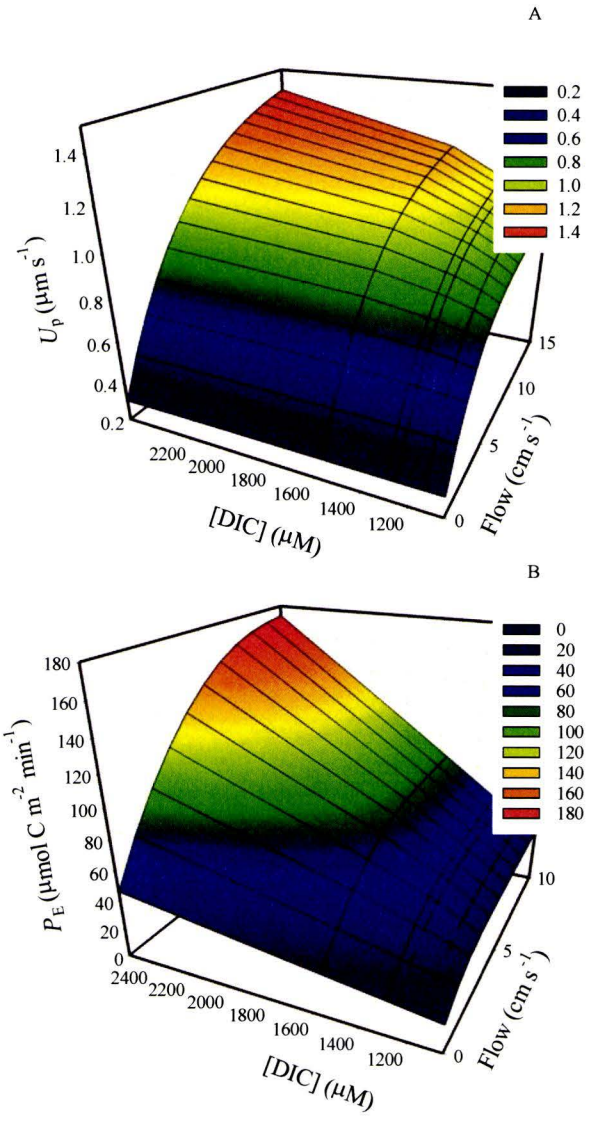

Fig. 5. A) Dependency of permeability (U_p) plotted as a function of [DIC] and flow [Eq. (6)]. B) Dependency of light-saturated photosynthesis (P_E) plotted as a function of [DIC] and flow [Eq. (3)].

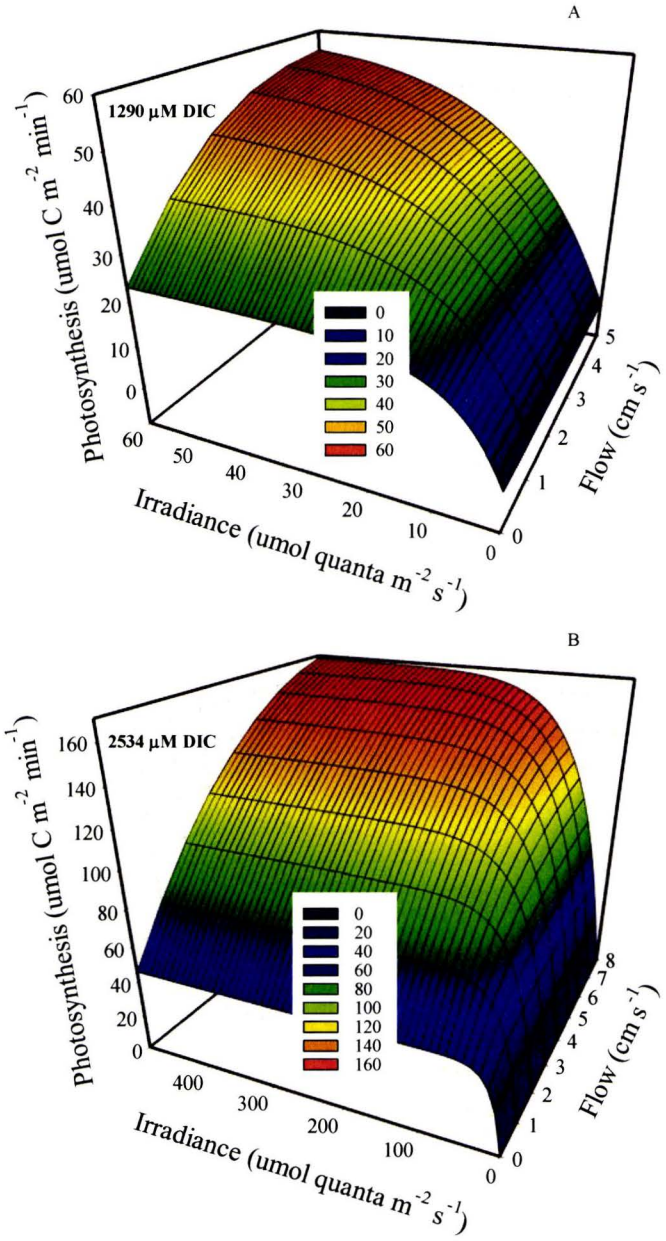

Fig. 6. (A) A three-dimensional representation of the combined influence of irradiance and flow on photosynthesis at ambient DIC conditions [Eq. (2); 1290 µM]. (B) A three-dimensional representation of the combined influence of irradiance and flow on photosynthesis at enriched DIC conditions [Eq. (2); 2534 µM].

Modeling Eelgrass Light Saturated $\delta^{13}C$ Signature

P_E/P_m increased non-linearly as a function of [DIC] and flow (Fig. 7) and ranged from 0.11 ([DIC] = 1059 μM; u = 0 cm s^{-1}) to 0.98 ([DIC] = 2533 μM; u = 20 cm s^{-1}). These two values served as the endmembers where carbon limited and carbon replete conditions, respectively, controlled isotopic discrimination at RUBISCO. Using the single linear relationship between P_E/P_m and theoretical photosynthetic ^{13}C fractionation, stable carbon isotope signatures were predicted across a range of environmental conditions (Fig. 8). Along with alkalinity, [DIC] controls the relative distributions of $CO_{2(aq)}$ and HCO_3^- in seawater, and these two form have characteristically different isotopic signatures [-9‰ and 0‰, respectively (Kroopnick 1985)]. At pH 6, 92% of [DIC] is [$CO_{2(aq)}$] versus only 0.01% at pH 8.1. However, differences in the distribution of DIC species had very little effect on $\delta^{13}C$ of the combined source, indicating that the distribution of inorganic carbon species in the source water didn't strongly influence on the overall stable carbon isotope signature of the leaf.

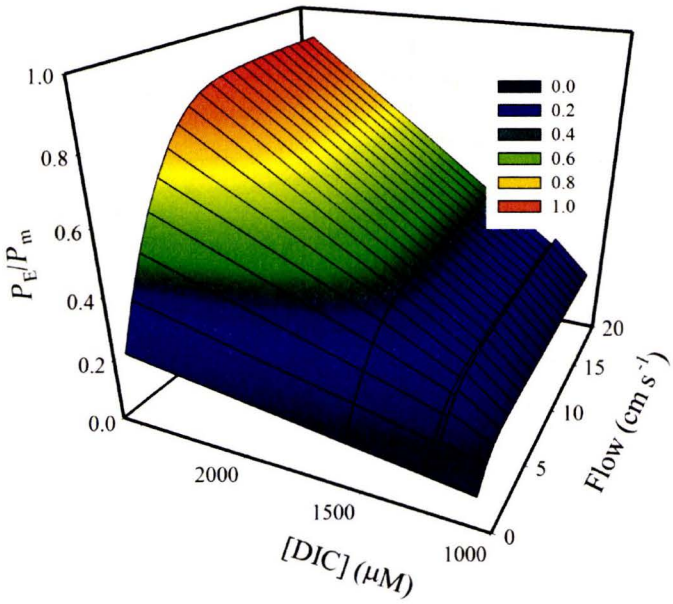

Fig. 7. The effect of flow and [DIC] on P_E/P_m. P_E/P_m represents the degree to which light-saturates photosynthesis (P_E) is saturated with respect to flow and [DIC]. When P_E/P_m =1, the supply of DIC exceeds demand and isotopic discrimination is controlled purely by RUBISCO.

Predicted values of light saturated $\delta^{13}C$ decreased nonlinearly with increasing flow and [DIC] (Fig. 9). Steepest gradients in predicted $\delta^{13}C$ signatures occurred when flow was saturated (>4 cm s-1) between carbon-limited (1000 μM) and carbon-replete (2500 μM) DIC concentrations. Predictions of $\delta^{13}C$ signatures for ambient [DIC] (Fig. 9; ~ 1290 μM ; ~ -7‰) and flow saturated (> 3 cm s^{-1}) conditions were well within the range of reported values across seagrass taxa [-23‰ to -3‰ (Hemminga and Mateo 1996)]. More importantly, predicted values from this study were consistent with values reported for light-saturated, carbon-limited environments [Carbon-limited fraction of the day > 0.8; measured turtlegrass $\delta^{13}C$ = ~ -7‰ (Hu et al. 2012)].

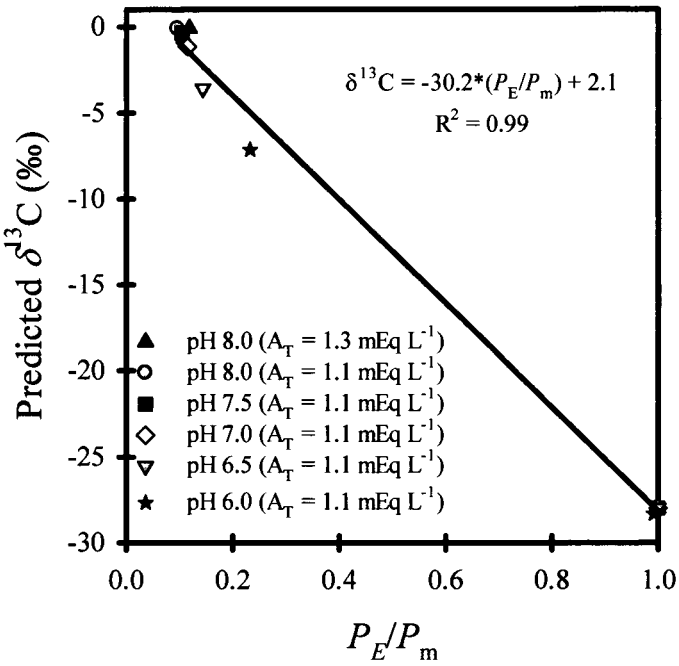

Fig. 8. The effect of P_E/P_m on $\delta^{13}C$ based on a simple linear mixing model. As P_E/P_m becomes limited by flow and/or [DIC], leaf $\delta^{13}C$ becomes increasingly defined by the isotopic composition and relative abundance of $[CO_{2(aq)}]$ and $[HCO_3^-]$ of the DIC source.

Stable Carbon Isotope Composition and the Environment

Understanding physiological and environmental processes that drive carbon uptake of eelgrass in nature is important for discerning trends in stable carbon isotope composition measured in the plant tissue across all submarine environments that vary in water column depth, optical properties, and hydrodynamics. This study took a

comparative approach between two very different light environments, temperate Goodwin Islands and subtropical Florida and Bahamas, and how the daily period of carbon limited photosynthesis influenced stable carbon isotope data across these two sites.

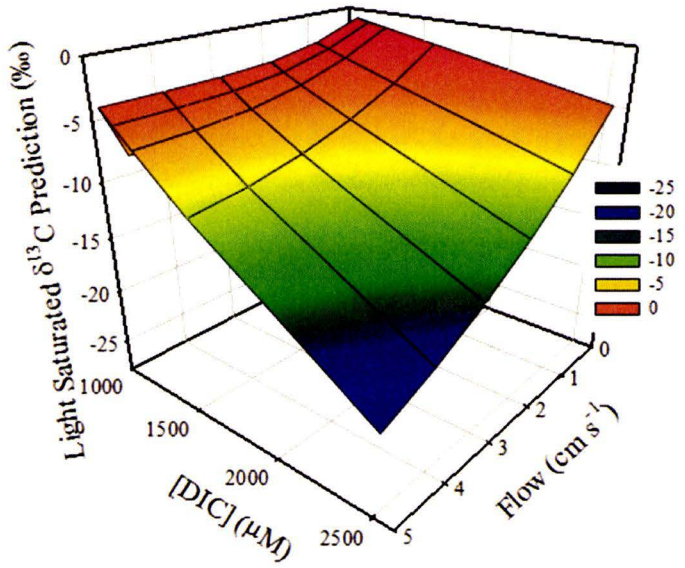

Fig. 9. A three-dimensional representation of the influence of flow on the light-saturated prediction of $\delta^{13}C$ signature based on the linear relationship shown in Fig. 8.

Time series of measured turbidity (NTU) from the NERRS data sonde at the Goodwin Islands field site averaged 3.5 NTU (± 0.14) during the period when eelgrass leaf samples were collected for $\delta^{13}C$ analysis. Although there was considerable variability in the Goodwin Islands moored data sonde turbidity measurements (shown by the subset of data in Fig. 10A), the relationship between daily mean turbidity and

measured $K_d(\lambda)$ was strongly linear (Fig. 10B; $R^2 = 0.83$; $p < 0.05$). Data sonde measurements had periodic high spikes, but $K_d(\lambda)$ predictions based on mean and median data were not significantly different. Additionally, measured and historically predicted $K_d(\lambda)$ based on mean turbidity data were statistically identical (Fig. 10C; ANOVA; $p < 0.05$) for all sampling days, allowing confidence in prediction of the historical light field for Goodwin Island remotely.

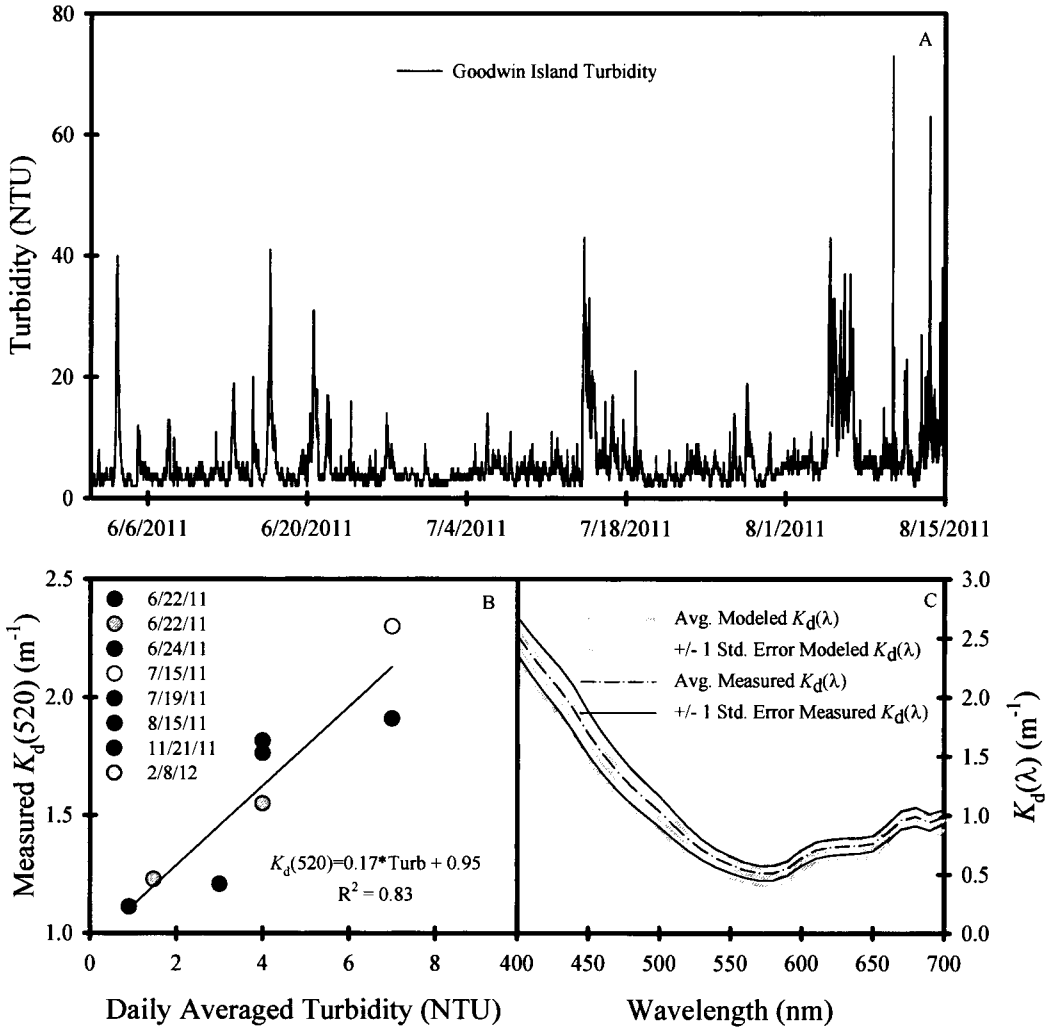

Fig. 10. A) A subset of Goodwin Island turbidity data collected from the NEERS data sonde plotted as a function of time. B) An example of the wavelength specific (520 nm) relationship between the diffuse attenuation for downwelling irradiance [K_d] from a variety of field excursions, determined using *Hydro-Rad 3*, plotted against corresponding daily median turbidity. C) Average modeled (based on K_d vs. turbidity relationship) and measured $K_d(\lambda)$ (*HR-3*) plotted against wavelength for all the days shown in (B).

With no apparent temporal (summer 2011 to winter 2012) or spatial (z = 0.1 m to 0.9 m) trend, Goodwin Islands stable carbon isotope signature ranged between -13.7‰ and -9.5‰. Since the plants grew at relatively shallow water depths across the entire

transect, without considering epiphytes the model predicted that most stations experienced light saturated photosynthesis for the entire day length (Carbon-limited P=; Fig. 11), and no significant relationship was found between the fraction of carbon limited photosynthesis and eelgrass $\delta^{13}C$ for Goodwin Island (p>0.01).

Based on long periods of light-saturated photosynthesis, $\delta^{13}C$ signatures of Goodwin Island eelgrass should be heavier than measured. The addition of modeled mean epiphyte loads, based on historical monthly data from Moore et al. [highest mean load in mid-summer (6.3 mg cm^{-2}) and lowest in the winter (1.9 mg cm^{-2}) (Moore 2004)], revealed significant reduction in the fraction of relative daily carbon limited photosynthesis. The stable carbon isotope signatures for eelgrass resembled values measured for *T. testudinum* measured for a similar range of relative daily carbon limited photosynthesis. When epiphytic cover was taken into account, the combined relationship between $\delta^{13}C$ and carbon limited photosynthesis for Goodwin Islands, Florida, and Bahamas remained statistically significant (Fig. 11; $R^2 = 0.55$; p<0.001). This suggests some commonality across seagrass species with regard to carbon isotope fractionation and $\delta^{13}C$.

Increasing light availability is the ultimate driver of photosynthesis and contributes (in addition to flow and DIC concentrations) to the rate of carbon uptake and fractionation at the site of RUBISCO by increasing carbon demand and decreasing fractionation. The mean water column depth across the eelgrass sampling gradient at Goodwin Islands was 0.5 m (SE ± 0.03), where Florida and Bahamas depths averaged 4.4 m (SE ± 0.3) and 5.9 m (SE ± 0.7), respectively (Fig.12), differences that can drive

spectral quality and quantity of light reaching the plant canopy. Average spectral light attenuation in the blue region of the spectrum [$K_d(440)$] was 3.4 and 13.8 times higher at Goodwin Islands than $K_d(440)$ measured from Florida and Bahamian stations, respectively (Hu et al. 2012). However, $K_d(\lambda)$ at the three locations converged at wavelengths of 550 nm and higher where Goodwin Islands was only 1.7 and 2.3 times higher than Florida and Bahamas, respectively (Fig.12A). Despite relatively high $K_d(\lambda)$ values at Goodwin Islands, average spectral downwelling irradiance [$E_d(\lambda)$] at the surface of the canopy across all stations at Goodwin Island was higher in the green and red than both Florida Bay and Bahamas (Fig.12B) because Goodwin Islands is shallow relative to the other two sites. However, Bahamian plants experienced the highest $E_d(440)$, approximately 1.5 times more than the other two sites. High $E_d(>500$ nm) incident on *Z. marina* plant canopies, relative to its subtropical counterparts, is explained simply by water column depth.

Based on field $\delta^{13}C$ data and modeled light saturated $\delta^{13}C$ signatures (discussed in the previous section), in addition to radiative transfer model calculations comparing eelgrass and turtlegrass, high epiphytic cover on Goodwin Islands eelgrass are undoubtedly causing light limitation.

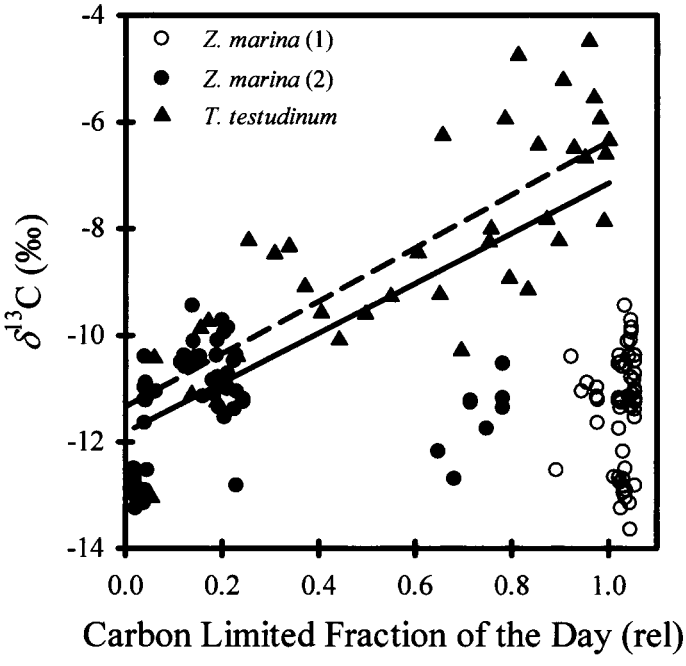

Fig. 11. Bahamian *T. testudinum* (Hu et al. 2012), Florida Bay *T. testudinum* (Campbell and Fourqurean 2009), and Goodwin Islands *Z. marina* δ^{13}C signature plotted as a function of the fraction of relative daily carbon limited photosynthesis. Goodwin Islands *Z. marina* shown for two different modeled epiphyte loads, (1) No epiphytes load added to model and (2) Epiphyte load based on historical monthly data (Moore 2004). The linear regression plotted for Florida and Bahamian *T. testudinum* (dash-dot line; $R^2 = 0.65$; $\delta^{13}C = 5.2 \cdot \mathrm{CLF} - 11.4$) and combined *T. testudinum* and Goodwin Islands *Z. marina* data based on historical monthly data from Moore (2004) (solid line; $R^2 = 0.55$; $\delta^{13}C = 4.7 \cdot \mathrm{CLF} - 11.8$).

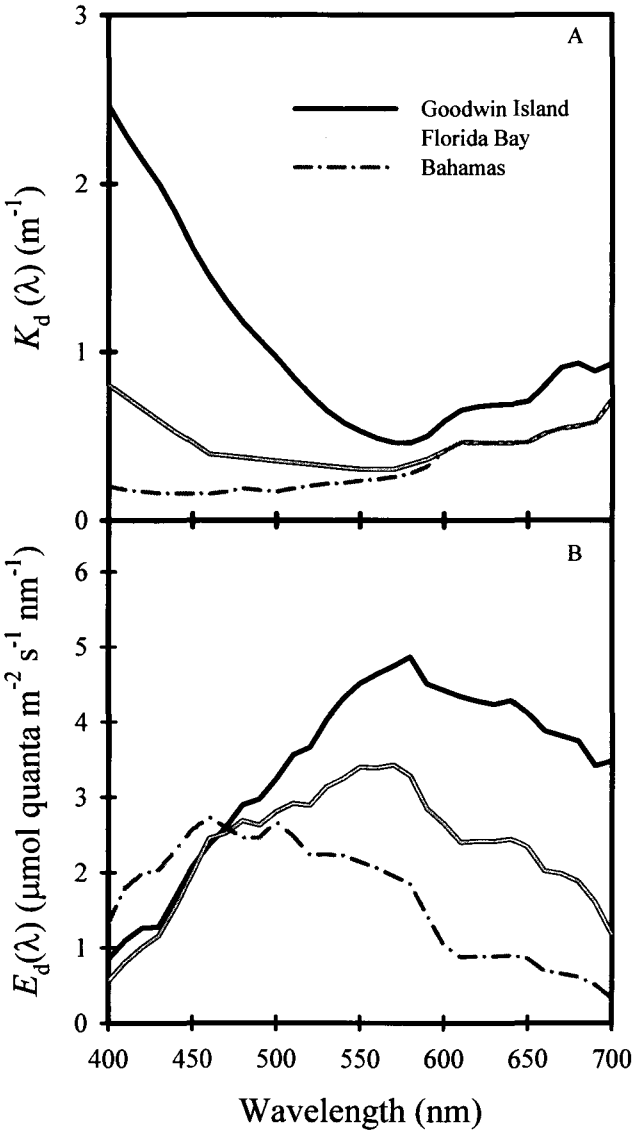

Fig.12. A) Site average $K_d(\lambda)$ for Goodwin Island, Florida Bay, and Bahamas at the top of the seagrass canopy. B) Site average $E_d(\lambda)$ for Goodwin Island, Florida Bay, and Bahamas at the top of the seagrass canopy.

CHAPTER IV

DISCUSSION

Modeling the effects of [DIC] and flow on P_E using the quadratic Hill-Whittingham equation predicted photosynthesis for a variety of parameters that most other general photosynthesis models ignore (Smith and Walker 1980) and validated the specific use of this more complex equation over other non-linear equations, such as Michaelis-Menton (Lucas 1975) and negative exponential curves (Zimmerman et al. 1987). Other less complex models may be sufficient for predicting photosynthesis in other marine autotrophs where carbon limitation poses little concern and increasing $[CO_{2(aq)}]$ has little effect on P_E (Raven et al. 1995), and in highly energetic flow environments (Koch et al. 2006; Mckone 2009). However, the ability of this more complex model to manipulate a variety of parameters for a seagrass system, including [DIC], flow, and permeability of the unstirred layer to predict carbon uptake provides a general mechanistic basis for predicting $\delta^{13}C$ that simpler formulations cannot accommodate. Predictions of stable carbon isotope signature were within the realm of expected values for a highly carbon-limited (light-saturated) seagrass population, but may differ for a range of light environments. High light conditions (inducing carbon-limited photosynthesis) decrease isotopic discrimination in seagrasses and result in heavier $\delta^{13}C$ signatures. High seawater [DIC] increases $CO_{2(aq)}$ availability to RUBISCO, increasing discrimination between ^{13}C and ^{12}C, which results in isotopically light $\delta^{13}C$ signatures. This study successfully modeled the complex interaction between [DIC], flow, and

permeability on $\delta^{13}C$ signature, however, the addition of light to $\delta^{13}C$ predictions proved challenging due to the inverse effects of light and [DIC] on isotopic fractionation. Understanding the inverse effects of these important environmental parameters on natural $\delta^{13}C$ signatures will become increasingly important for understanding carbon uptake by seagrasses in response to future changing environmental conditions, including climate change and coastal eutrophication.

Additionally, based on these model results, seagrass populations in high flow areas may benefit more from predicted future inorganic carbon conditions because of steep gradients between flow-saturated and flow-limited photosynthesis at high [$CO_{2(aq)}$]. However, seagrasses growing in low flow environments, such as dense seagrass beds (Peterson et al. 2004a) or sheltered coastal bays (Hurd 2000), will still benefit greatly from increased carbon dioxide concentrations since increased dependence on $CO_{2(aq)}$ over HCO_3^- at flow limited velocities was responsible for increases in the changing slope of flow-dependent photosynthesis (Fig. 5 and Fig. 6).

Submerged aquatic vegetation (SAV) reduce and attenuate wave energy, and plant canopy shape and shoot density are population-level factors that influence the flow of water through, and boundary layer conditions within, the seagrass canopy (Fonseca and Koehl 2006; Koch et al. 2006; Peterson et al. 2004b). High density beds are particularly sensitive to hydrodynamic conditions because flow reduction increases boundary layer conditions within the canopy (Koch 2001; Mckone 2009), which flume studies proved has profound effects on individual leaf photosynthetic rates at flows less than 4 cm s^{-1}. Flow regimes within a seagrass meadow distinctly differs between tide-

and wave-dominated systems and can greatly influence the flux of carbon into a seagrass canopy (Koch and Gust 1999). Water movement through relatively sparse seagrass beds at Goodwin Islands is likely influenced by both tidal fluctuations and wave oscillations (Orth et al. 2006b), therefore seagrass photosynthesis and carbon uptake is unlikely flow limited and isotopic fractionation affected little by boundary layer conditions restricting the supply of inorganic carbon to the leaf surface.

Approximately 17 out of 50 species of seagrasses use bulk HCO_3^- for photosynthesis and it is argued that this physiological adaptation is important for a submerged aquatic life history (Beer 1989; Campbell 2012). However, experiments conducted here for the influence of CA on HCO_3^- uptake over a variety of flows using AZ did not show a significant difference between photosynthesis measurements with and without the addition of AZ, contradictory to some studies conducted on *Z. marina* at pH 8.1 which showed a 20 to 50% depression in photosynthesis (Hellblom et al. 2001; Zimmerman pers. comm). Based on Hill-Whittingham model calculations and data shown in Fig. 3, Goodwin Islands eelgrass must be using $CO_{2(aq)}$ and HCO_3^- because: 1) HCO_3^- usage increased and $CO_{2(aq)}$ usage decreased as flow increased (Fig. 3B); 2) modeled calculations based on $[CO_{2(aq)}]$ under-predicted measured photosynthesis values (Fig. 3A); and 3) calculated permeability of the unstirred layer based on $[CO_{2(aq)}]$ was three orders of magnitude greater than literature reported values of 0.6 $\mu m\ s^{-1}$ (Fig. 3C) (Smith and Walker 1980). The photosynthetic insensitivity to AZ suggests that CA was unimportant for HCO_3^- utilization in Goodwin Islands eelgrass, in addition to strong

evidence that both HCO_3^- and $CO_{2(aq)}$ were utilized by these plants, suggests additional pathways to HCO_3^- use other than dehydration by CA.

Three pathways are widely considered to dominate inorganic carbon utilization in aquatic autotrophs, ultimately by diffusion across the leaf surface: 1) mediated extracellular CA conversion of HCO_3^- to $CO_{2(aq)}$, but limited by the equilibrium restraints of seawater pH; 2) mediated extracellular CA conversion of HCO_3^- to $CO_{2(aq)}$, where seawater pH within the boundary layer and cell wall is altered by proton pumps within the plasma membrane; and 3) active acidification of the boundary layer and cell wall by proton pumps, while relying on seawater equilibrium constraints to control conversion of HCO_3^- to $CO_{2(aq)}$ (Beer et al. 2002; Larkum et al. 2006). Systems 1 and 2 are sensitive to AZ addition because CA inhibition blocks conversion of HCO_3^-. Subsequently, HCO_3^- dehydration, via proton pumping, cannot be ruled out as an important mechanism for carbon uptake in Goodwin Islands eelgrass (Beer et al. 2006; Beer et al. 2002; Hellblom et al. 2001).

Identifying processes of inorganic carbon uptake is an important puzzle piece for determining controlling factors of stable carbon isotope signature in seagrasses. It can be implied from this study, that inorganic carbon utilization mechanisms may vary within species depending on seawater chemistry conditions (Hellblom et al. 2001), such as pH and [DIC]. Seagrasses are generally considered to use HCO_3^- as a significant inorganic carbon source at ambient pH (Beer and Rehnberg 1997; Durako 1993; Invers et al. 2001; Millhouse and Strother 1986), contributing to relatively heavy $\delta^{13}C$ signatures across all

species (-23 to -3 ‰) (Hemminga and Mateo 1996). Population-specific use of HCO_3^- may further influence variations of $\delta^{13}C$ within and among seagrass species (Campbell and Fourqurean 2009). Additionally, the extent to which HCO_3^- is used depends on a variety of factors including [$CO_{2(aq)}$] (Beer et al. 2002), light availability (Hu et al. 2012), and current velocity.

Measured Goodwin Islands eelgrass $\delta^{13}C$ values (mean = -11.4 ‰ ± 0.14) were mostly at the ^{13}C depleted end of the range for this species (-12.4 to -6 ‰) (Hemminga and Mateo 1996), and based on the linear relationship between $\delta^{13}C$ and daily fraction of carbon limited photosynthesis from Hu et al. (Hu et al. 2012), suggested that photosynthesis of this population was largely light limited (Fig. 11). Several environmental factors can negatively influence productivity rates at this site, including, light availability and quality (Fig.12) (Kirk 1994; Moore et al. 1996), canopy height and density (Gruber et al. 2011; Zimmerman 2003b), high summertime temperatures, and epiphyte loading (Bulthuis and Woelkerling 1983; Koch et al. 2006). The environmental stresses experienced by seagrass at Goodwin Islands most likely played an important role in the relatively scattered $\delta^{13}C$ signatures measured across time and space (Fig. 11). The simulation of light reduction based on historical epiphyte loads brought Goodwin Islands eelgrass $\delta^{13}C$ signatures into the range of expected values modeled for *T. testudinum* (Hu et al. 2012). This indicated that epiphytes may play a significant role in the ecology of nutrient enriched seagrass communities, and the importance of the complex interactions between top-down (predators) and bottom-up (nutrient loading and water quality) effects on seagrass grown and ecosystem functions (Hughes et al. in prep). High summer-time

temperatures (Moore et al. 2012) and epiphyte loads (Moore 2004) reduce light, driving eelgrass survival to depths less than 1 m, and cause canopy densities to fluctuate seasonally. Additionally, epiphytes restrict plants to shallow depths where they become particularly vulnerable to other stressors, including storm surge.

Seagrasses are particularly vulnerable to a host of anthropogenic influences that plague coastal ecosystems around the globe (Orth et al. 2006a). There is increasing demand, from managers and scientists, for a simple and inexpensive tool that can associate a variety of important parameters (light availability, productivity, environmental conditions, etc.) controlling the health of seagrass beds. Understanding the fundamental mechanisms governing the relationship between photosynthesis and $\delta^{13}C$ are critical in present changing coastal environmental conditions and will be important for modeling future changes in seagrass ecosystems. In addition, this information will be important to understand physiological responses of seagrasses from increasing temperature and $[CO_{2(aq)}]$ as a result of climate change.

Owing to seagrasses inherent high light and carbon requirements across all seagrass genera, modeling and monitoring with $\delta^{13}C$ is widely applicable. The ability to model productivity and $\delta^{13}C$ signatures of a seagrass population accurately suggests a comprehensive understanding of the relationship between light availability, photosynthesis, and carbon acquisition in these organisms and shows significant improvement in our knowledge of specific environmental conditions influencing carbon uptake in these plants.

REFERENCES

Beer, S. 1989. Photosynthesis and photorespiration of marine angiosperms. Aquatic Botany **34:** 153-166.

Beer, S., L. Axelson, and M. Bjork. 2006. Modes of photosynthetic bicarbonate utilisation in seagrasses, and their possible roles in adaptations to specific habitats. *In* M. C. Gambi et al. [eds.], Mediterranean Seagrass Workshop.

Beer, S., M. Bjork, F. Hellblom, and L. Axelsson. 2002. Inorganic carbon utilization in marine angiosperms (seagrasses). Funct. Plant Biol. **29:** 349-354.

Beer, S., and J. Rehnberg. 1997. The acquisition of inorganic carbon by the seagrass *Zostera marina*. Aquatic Botany **56:** 277-283.

Bjork, M., A. Weil, S. Semesi, and S. Beer. 1997. Photosynthetic utilisation of inorganic carbon by seagrasses from Zanzibab, East Africa. Marine Biology **129:** 363-366.

Bulthuis, D. A., and W. J. Woelkerling. 1983. Biomass accumulation and shading effects of epiphytes on leaves of the seagrass, *Heterozostera tasmanica*, in Victoria, Australia. Aquatic Botany **16:** 137-148.

Campbell, J. E. 2012. The Effects of Carbon Dioxide Fertilization on the Ecology of Tropical Seagrass Communities. Florida International University.

Campbell, J. E., and J. W. Fourqurean. 2009. Interspecific variation of the elemental and stable isotope content of seagrasses in South Florida. Marine Ecology Progress Series **387:** 109-123.

Cooper, L. W., and M. J. Deniro. 1989. Stable carbon isotope variability in the seagrasses *Posidonia oceanica*: evidence for light intensity effects. Mar. Ecol. Prog. Ser. **50:** 225-229.

Denny, M. W. 1993. Air and Water. Princeton University Press.

Duarte, C. M. 1991. Seagrass depth limits. Aquatic Botany **40:** 363-377.

Durako, M. J. 1993. Photosynthetic utilization of $CO_{2(aq)}$ and HCO_3^- in *Thalassia testudinum* (Hydrocharitaceae). Marine Biology **115:** 373-380.

Evans, A. S., K. L. Webb, and P. A. Penhale. 1986. Photosynthetic temperature acclimation in two coexisting seagrasses, Zostera marina L. and Ruppia maritima L. Aquatic Botany **24:** 185-197.

Falkowski, P. G., and J. A. Raven. 2007. Aquatic Photosynthesis, 2nd ed. Princeton University Press.

Fonseca, M. S., and M. a. R. Koehl. 2006. Flow in seagrass canopies: The influence of patch width. Estuarine, Coastal and Shelf Science **67:** 1-9.

Fourqurean, J., S. Escorcia, W. Anderson, and J. Zieman. 2005. Spatial and seasonal variability in elemental content, $\delta^{13}C$ and $\delta^{15}N$ of *Thalassia testuninum* from South Florida and its implications for ecosystem studies. Estuaries and Coasts **28:** 447-461.

France, R. L. 1995. Carbon-13 enrichment in benthic compared to planktonic algae: foodweb implications. Mar. Ecol. Prog. Ser. **124:** 307-312.

Gieskes, J. M., and W. C. Rogers. 1973. Alkalinity Determination in Interstitial Waters of Marine Sediments. Journal of Sediment Research **43:** 272-277.

Grice, A. M., N. R. Loneragan, and W. C. Dennison. 1996. Light intensity and the interactions between physiology, morphology and stable isotope ratios in five species of seagrass. Journal of Experimental Marine Biology and Ecology **195:** 91-110.

Gruber, R. K., D. C. Hinkle, and W. M. Kemp. 2011. Spatial Patterns in Water Quality Associated with Submersed Plant Beds. Estuaries and Coasts **34:** 961-972.

Hellblom, F., S. Beer, M. Bjork, and L. Axelsson. 2001. A buffer-sensitive inorganic carbon utilization system in *Zostera marina.* . Aquatic Botany **69:** 55-62.

Hellblom, F., and M. Björk. 1999. Photosynthetic responses in Zostera marina to decreasing salinity, inorganic carbon content and osmolality. Aquatic Botany **65:** 97-104.

Hemminga, M. A., N. Marba, and J. Stabel. 1999. Leaf nutrient resorption, leaf lifespan and the retention of nutrients in seagrass systems. Aquatic Botany **65:** 141-158.

Hemminga, M. A., and M. A. Mateo. 1996. Stable carbon isotopes in seagrasses: variability in ratios and use in ecological studies. Mar. Ecol. Prog. Ser. **140:** 285-298.

Hill, R., and C. P. Whittingham. 1955. Photosynthesis. Methuen.

Hu, X., D. J. Burdige, and R. C. Zimmerman. 2012. $\delta^{13}C$ is a signature of light availability and photosynthesis in seagrass. Limnol. and Oceanogr. **57:** 441-448.

Hughes, B. B., R. Eby, E. Van Dyke, K. Wasson, and C. Marks. in prep. Sea otters mediate negative eutrophication effects on seagrass through a multi-level trophic cascade.

Hurd, C. L. 2000. Water motion, marine macroalgae physiology, and production. Journal of Phycology **36:** 453-472.

Invers, O., M. Pérez, and J. Romero. 1999. Bicarbonate utilization in seagrass photosynthesis: role of carbonic anhydrase in Posidonia oceanica (L.) Delile and Cymodocea nodosa (Ucria) Ascherson. Journal of Experimental Marine Biology and Ecology **235:** 125-133.

Invers, O., R. C. Zimmerman, R. S. Alberte, M. Perez, and J. Romero. 2001. Inorganic carbon sources for seagrass photosynthesis: an experimental evaluation of bicarbonate use in species inhabiting temperate waters. Journal of Experimental Marine Biology and Ecology **265:** 203-217.

James, P. L., and A. W. D. Larkum. 1996. Photosynthetic inorganic carbon acquisition of *Posidonia australis.* Aquatic Botany **55:** 149-157.

Kirk, J. T. 1994. Light and Photosynthesis in Aquatic Ecosystems, 2nd edition ed. Cambridge University Press.

Koch, E. 2001. Beyond light: Physical, geological, and geochemical parameters as possible submersed aquatic vegetation habitat requirements. Estuaries and Coasts **24:** 1-17.

Koch, E., J. Ackerman, J. Verduin, and M. Keulen. 2006. Fluid Dynamics in Seagrass Ecology—from Molecules to Ecosystems, p. 193-225. *In* A. W. D. Larkum, R. J. Orth and C. M. Duarte [eds.], Seagrasses: Biology, Ecology and Conservation. Springer.

Koch, E. W., and G. Gust. 1999. Water flow in tide- and wave-dominated beds of the seagrass *Thalassia testudinum*. Mar. Ecol. Prog. Ser. **184:** 63-72.

Kroopnick, P. M. 1985. The distribution of 13C of ΣCO2 in the world oceans. Deep Sea Research Part A. Oceanographic Research Papers **32:** 57-84.

Larkum, A., E. Drew, and P. Ralph. 2006. Photosynthesis and Metabolism in Seagrasses at the Cellular Level, p. 323-345. *In* A. W. D. Larkum, R. J. Orth and C. M. Duarte [eds.], Seagrasses: Biology, Ecology and Conservation. Springer.

Lewis, D. E., and D. W. R. Wallace. 2006. MS. Program Developed for CO_2 system calculations. Oak Ridge National Laboratory.

Lucas, W. J. 1975. Photosynthetic Fixation of 14Carbon by Internodal Cells of Chara corallina. Journal of Experimental Botany **26:** 331-346.

Maberly, S. C., J. A. Raven, and A. M. Johnston. 1992. Discrimination between ^{12}C and ^{13}C by marine plants. Oecologia **91:** 481-492.

Madsen, T. V., and K. Sand-Jensen. 1991. Photosynthetic carbon assimilation in aquatic macrophytes. Aquatic Botany **41:** 5-40.

Mckone, K. L. 2009. Light Available to the seagrass *Zostera marina* when exposed to currents and waves. University of Maryland, College Park.

Millhouse, J., and S. Strother. 1986. The effect of pH on the inorganic carbon source for photosynthesis in the seagrass *Zostera muelleri* irmisch ex aschers. Aquatic Botany **24:** 199-209.

Moore, K. A. 2004. Influence of Seagrasses on Water Quality in Shallow Regions of the Lower Chesapeake Bay. Journal of Coastal Research **45:** 162-178.

Moore, K. A., H. A. Neckles, and R. J. Orth. 1996. *Zostera marine* (eelgrass) growth and survival along a gradient of nutrients and turbidity in the lower Chesapeake Bay. Marine Ecology Progress Series **142:** 247-259.

Moore, K. A., E. C. Shields, D. B. Parrish, and R. J. Orth. 2012. Eelgrass survival in two contrasting systems: role of turbidity and summer water temperatures. Mar. Ecol. Prog. Ser. **448:** 247-258.

O'leary, M. H. 1981. Carbon Isotope Fractionation in Plants. Phytochemistry **20:** 553-567.

Orth, R. J. and others 2006a. A Global Crisis for Seagrass Ecosystems. Bioscience Magazine **56:** 987-995.

Orth, R. J., K. A. Moore, B. Anderson, S. Marion, and D. Wilcox. 2006b. Restoration of seagrasses in Virginia Coastal Bays - Year 3. Virginia Institute of Marine Science, College of William and Mary.

Palacios, S. L., and R. C. Zimmerman. 2007. Response of eelgrass *Zostera marina* to CO_2 enrichment: possible impacts of climate change and potential for remediation of coastal habitats. Mar. Ecol. Prog. Ser. **344:** 1-13.

Penhale, P. A. 1977. Macrophyte-epipyte biomass and productivity in an eelgrass (*Zostera marina* L.) community. J. Exp. Mar. Biol. Ecol. **26:** 211-224.

Peterson, B. J., and B. Fry. 1987. Stable Isotopes in Ecosystem Studies. Annual Review of Ecology and Systematics **18:** 293-320.

Peterson, C. H., R. A. Luettich, F. Micheli, and G. A. Skilleter. 2004a. Attenuation of water flow inside seagrass canopies of differing structure. Mar. Ecol. Prog. Ser. **268:** 81-92.

---. 2004b. Attenuation of water flow inside seagrass canopies of differing structure. Marine Ecology Progress Series **268:** 81-92.

Raven, J. A. and others 2002. Mechanistic interpretation of carbon isotop discrimination by marine macroalgae and seagrasses. Funct. Plant Biol. **29:** 355-378.

Raven, J. A., N. A. Walker, A. M. Johnston, L. L. Handley, and J. E. Kubler. 1995. Implications of ^{13}C natural abundance measurements for photosynthetic performance by marine macrophytes in their natural environment. Mar. Ecol. Prog. Ser. **123:** 193-205.

Sharp, Z. 2007. Principles of stable isotope geochemistry. Pearson/Prentice Hall.

Smith, B. N., and S. Epstein. 1971. Two Catagories of $^{13}C/^{12}C$ Ratios for Higher Plants. Plant Physiol. **47:** 380-384.

Smith, F. A., and N. A. Walker. 1980. Photosynthesis by aquatic plants: Effects of unstirred layers in relation to assimilation of CO_2 and HCO_3^- and to carbon isotopic discrimination. New Phycol. **86:** 245-259.

Webb, W. L., M. Newton, and D. Starr. 1974. Carbon dioxide exchange of *Alnus rubra.* Oecologia **17:** 281-291.

Zeebe, R. E., and D. A. Wolf-Gladrow. 2003. CO_2 in Seawater: Equilibrium, Kinetics, Isotopes. Elsevier.

Zhang, J., P. D. Quay, and D. O. Wilbur. 1995. Carbon isotope fractionation during gas-water exhange and dissolution of CO_2. Geochimica et Cosmochimica Acta **59:** 107-114.

Zimmerman, R. C. 2003a. Appendix M. Final Report: A bio-physical model evaluation of eelgrass distribution and habitat potential in Dumas Bay, WA. *In* H. D. Berry et al. [eds.].

Zimmerman, R. C. 2003b. A biooptical model of irrandiance distribution and photosynthesis in seagrass canopies. Limnology and Oceanography **48:** 568-585.

Zimmerman, R. C. pers. comm. Bicarbonate utilization through carbonic anhydrase dependent uptake in *Z. marina. In* M. L. McPherson [ed.].

Zimmerman, R. C., and A. G. Dekker. 2006. Chapter 12. Aquatic Optics: Basic Concepts for Understanding How Light Affects Seagrasses and Makes them Measurable from Space, p. 295-301. *In* A. W. D. Larkum [ed.], Seagrasses: Biology, Ecology, and Conservation. Springer.

Zimmerman, R. C., D. G. Kohrs, D. L. Steller, and R. S. Alberte. 1997. Impacts of CO2 Enrichment on productivity and light requirements of Eelgrass. Plant Physiol. **115:** 599-607.

Zimmerman, R. C., J. L. Reguzzoni, S. Wyllie-Echeverria, M. Josselyn, and R. S. Alberte. 1991. Assessment of environmental suitability for growth of Zostera marina L. (eelgrass) in San Francisco Bay. Aquatic Botany **39:** 353-366.

Zimmerman, R. C., J. B. Soohoo, J. N. Kremer, and D. Z. D'argenio. 1987. Evaluation of variance approximation techniques for non-linear photosynthesis-irradiance models. Marine Biology **95:** 209-215.

VITA

MEREDITH LEIGH MCPHERSON
Department of Ocean, Earth, and Atmospheric Sciences
Old Dominion University
Norfolk,VA 23529

Meredith Leigh McPherson was born in . Upon graduating from high school in Yorktown, VA in 2004, she attended Old Dominion University (ODU) to obtain a double BS in Biology and Ocean, Earth, and Atmospheric Sciences. In 2007, Meredith joined Dr. Richard Zimmerman's Bio-Optical Research Group (BORG) as an undergraduate research assistant and conducted research under an ODU Honors College undergraduate research grant. While an undergraduate, Meredith was an athlete on the school's competitive club rowing team between 2004 through 2008, and served as treasurer and vice-president. In 2008, Meredith joined the Women's Varsity rowing team from 2008 to 2009 on an athletic scholarship and was awarded best All-Around Athlete. Throughout her rowing career she won several national championship titles. Following the completion of her BS in 2009, she continued on as a graduate student in Dr. Zimmerman's lab. Between August 2009 and May 2011, she was assigned to the undergraduate Oceanography capstone course as a graduate teaching assistant. During her MS, she authored one featured peer-reviewed publication in the journal *Estuaries and Coasts*, and presented at 5 international meetings. Meredith also received 7 scholarships, which included travel grants, research grants, and a study grant.